



# RAD-NNET, a neural network based correlation developed for a realistic simulation of the non-gray radiative heat transfer effect in three-dimensional gas-particle mixtures

Walter W. Yuen\*

Department of Mechanical Engineering, University of California at Santa Barbara, Santa Barbara, CA 93106, USA

## ARTICLE INFO

### Article history:

Received 16 November 2007  
 Received in revised form 23 January 2009  
 Accepted 23 January 2009  
 Available online 30 March 2009

## ABSTRACT

A neural network correlation, RAD-NNET, is developed to simulate the realistic effect of non-gray radiative absorption by a homogeneous mixture of combustion gases ( $\text{CO}_2$  and  $\text{H}_2\text{O}$ ) and soot using numerical data generated by RADCAL. RAD-NNET is then applied to assess the accuracy of some commonly accepted approximate approaches to evaluate radiative heat transfer in three-dimensional non-gray media. Results show that there are significant errors associated with the current approximate approaches. RAD-NNET can be readily implemented in commercial CFD codes to greatly enhance the accuracy of simulation of radiative heat transfer in practical engineering systems.

© 2009 Elsevier Ltd. All rights reserved.

## 1. Introduction

Over the past 50 years, many important advances have been made both in computational techniques for multi-dimensional radiative transfer and the understanding of spectroscopic absorption properties of different combustion gases [1,2]. Reasonably accurate experimental data and computational results for radiative absorption and emission by non-isothermal, inhomogeneous, non-gray gas/particulate mixture are now available in the literature [3,4]. Effects of scattering are also included in many studies [5]. However, few of these research advances have been utilized in any significant degree by the engineering design/safety community, particularly in the areas of combustion/fire, where the effective of radiation is known to be not only important, but dominant. For example, in both simplified one-zone computational code (e.g. CFAST [6]) and multi-dimensional CFD codes (e.g. FDS [7] and FLUENT) developed for application in practical fire/combustion systems, the simulation of the radiation effect is still largely limited to the utilization of one-dimensional empirical charts/correlations [8]. The multi-dimensional geometric effect is accounted for by the traditional mean beam length concept developed by Hottel [9] and the utilization of some ad-hoc length scales without mathematical validation [10]. Currently, the lack of a simple-to-use and mathematically validated methodology which would allow non-experts in radiation to implement the correct physics of radiative transfer into practical engineering design calculation is a serious

obstacle to the design/safety community in understanding the effect of radiative heat transfer.

The objective of this work is to demonstrate that the concept of neural network is ideally suited as a tool to implement the complex radiative absorption/emission data into an actual engineering calculation, accounting for all important physical effects both accurately and efficiently. Fundamentally, neural network is a branch of computer science that uses interconnected processing elements called neurons to either simulate or analyze complex phenomena [11]. It has been used extensively in many disciplines including biomedical research, geophysical science, as well as non-scientific fields such as banking and insurance analysis (see Ref. [12] for a list of various neural network applications). In heat transfer, the concept of neural network has also been used extensively in areas such as retrieval of optical properties [13–15], inverse heat transfer problems [16–18] and heat exchanger applications [19]. But in contrast to many of these existing applications, the objective the current radiation neural network, RAD-NNET, is not to “predict” new radiative absorption/emission information outside of the parametric ranges within which the existing data were obtained. Instead, RAD-NNET is used to “recover” existing radiative absorption/emission data efficiently and accurately for application in a larger, more complex engineering calculation. Mathematically, it can be proved rigorously that with an appropriate of layer structure and sufficient number of neurons, a neural network can approximate any mathematical functions to a high degree of accuracy with no restriction on the number of independent and dependent variables [20]. Any physical phenomenon which can be formulated generally as a mathematical relation between a set of input variables and a set of output variables, can thus be repre-

\* Tel.: +1 805 893 3892; fax: +1 805 893 8651.  
 E-mail address: [yuen@engineering.ucsb.edu](mailto:yuen@engineering.ucsb.edu)



### Three Layers of Neurons

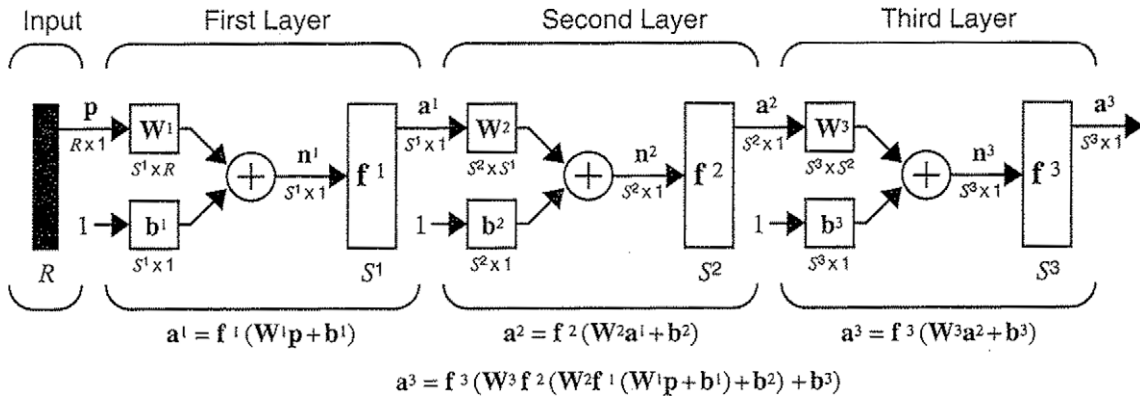


Fig. 1. Structure of a three-layer neural network used in the correlation of the excess absorptivity,  $\Delta\alpha(T_w, T_g, P_{CO_2} L, P_{H_2O} L, f_v L)$ .

$$\begin{aligned}
 0 &\leq P_g L \leq 1000 \text{ kPa m}, & P_g &= P_{CO_2} + P_{H_2O} \\
 0 &\leq F_{CO_2} \leq 1.0, & F_{CO_2} &= \frac{P_{CO_2}}{P_g} \\
 0 &\leq f_v L \leq 10^{-6} \text{ m} \\
 300K &\leq T_w, T_g \leq 2000 \text{ K}
 \end{aligned}
 \tag{5}$$

Because the total gas pressure is assumed to be 100 kPa,  $L$  is assumed to be 1 m in the generation of numerical data in the range of  $P_g L \leq 100$  kPa-m while  $L$  is assumed to be 10 m in the range of  $P_g L \geq 100$  kPa-m. Absorptivity data are generated over 550 discrete value of  $P_g L$ , 11 discrete value of  $F_{CO_2}$ , 10 discrete value of  $f_v L$ , 13 discrete value of  $T_w$  and  $T_g$ , respectively, corresponding to a set of over 10 million data points. In general, the data are distributed evenly over the range of the input variable space. Numerical experiments show that the number of data point is sufficient and the distribution is well distributed to generate an accurate neural network for the data set.

Even though there's no restriction on the size of the data set and the number of variables used in the development of a neural network, the development process can be made more efficient if the data set can be re-organized using physical and mathematical consideration. For example, using the Rayleigh small-particle limit of the absorption coefficient as shown in Eq. (3), the absorptivity due to soot only can be readily integrated to yield [1]

$$\alpha_s(T_w, f_v L) = \frac{\int_0^\infty e_{ib}(T_w)(1 - e^{-a_s L})}{\sigma T_w^4} = 1 - \frac{15}{\pi^4} \psi^{(3)}\left(1 + \frac{cLT_w}{C_2}\right) \tag{6}$$

with  $C_2$  being the second radiation constant and  $\psi^{(3)}(z)$  is the pentagram function for which tabulated values are available. Since the effect of soot absorption can be readily evaluated by Eq. (6), it is computationally efficient to develop a neural network only for the “excess absorptivity” given by

$$\Delta\alpha(T_w, T_g, P_g L, F_{CO_2}, f_v L) = \alpha(T_w, T_g, P_g L, F_{CO_2}, f_v L) - \alpha_s(T_w, f_v L) \tag{7}$$

Note that  $\Delta\alpha$  is still a function of five independent variables including the soot volume fraction  $f_v L$  because the total absorptivity is not linearly separable into a “soot” component and a “gas” component. In the limit of zero soot volume fraction,  $\Delta\alpha$  is the total gas absorptivity.

Since the gaseous optical thickness  $P_g L$  is expected to have the most significant effect on the behavior of  $\Delta\alpha$ , the input optical thickness space is separated into 10 distinct regions in the generation of the neural network. Numerical experiments show that this is effective in reducing the size of the neural network needed for an

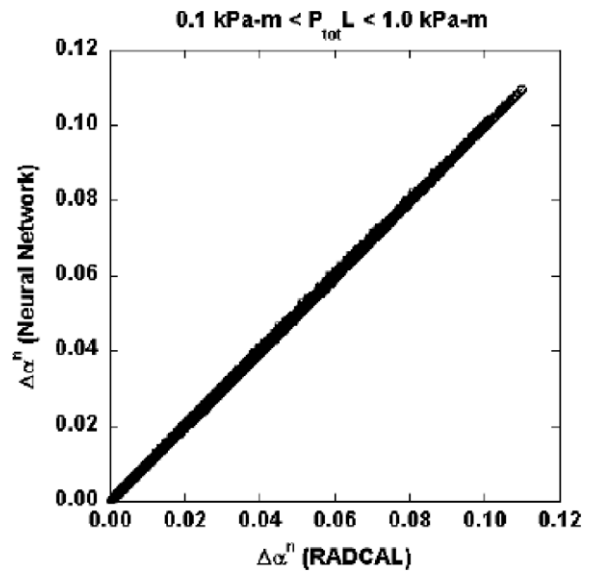


Fig. 2. Comparison between the neural network prediction and the RADCAL results for the region  $0.1 \text{ kPa m} < P_g L < 1.0 \text{ kPa m}$ .

accurate simulation of the numerical data in each of the considered optical thickness region. Specifically, neural networks for  $\Delta\alpha$  are first generated for eleven specific values of the  $P_g L$  (0.01, 0.05, 0.1, 0.5, 1.0, 5.0, 10.0, 50.0, 100.0, 300.0 and 1000.0 kPa-m). For the 10 intermediate regions, neural networks are generated for the normalized “excess absorptivity” given by

Table 1  
Dimension of the weighting matrix and bias vector for the six neural networks with constant gaseous optical thicknesses.

| $P_g L$ (kPa m) | $N$ | $S_1$ | $S_2$ | $S_3$ |
|-----------------|-----|-------|-------|-------|
| 0.01            | 4   | 9     | 6     | 1     |
| 0.05            | 4   | 15    | 8     | 1     |
| 0.1             | 4   | 15    | 9     | 1     |
| 0.5             | 4   | 17    | 14    | 1     |
| 1.0             | 4   | 17    | 11    | 1     |
| 5.0             | 4   | 15    | 10    | 1     |
| 10.0            | 4   | 15    | 10    | 1     |
| 50.0            | 4   | 16    | 12    | 1     |
| 100.0           | 4   | 16    | 12    | 1     |
| 300.0           | 4   | 16    | 12    | 1     |
| 1000.0          | 4   | 17    | 13    | 1     |

**Table 2**  
Dimension of the weighting matrix and bias vector for the neural networks of the five regions of optical thicknesses.

| $P_g L$ (kPa m) | $N$ | $S_1$ | $S_2$ | $S_3$ |
|-----------------|-----|-------|-------|-------|
| 0.01–0.05       | 5   | 8     | 5     | 1     |
| 0.05–0.1        | 5   | 5     | 3     | 1     |
| 0.1–0.5         | 5   | 7     | 4     | 1     |
| 0.5–1.0         | 5   | 6     | 4     | 1     |
| 1.0–5.0         | 5   | 9     | 5     | 1     |
| 5.0–10.0        | 5   | 7     | 4     | 1     |
| 10.0–50.0       | 5   | 8     | 5     | 1     |
| 50.0–100.0      | 5   | 8     | 5     | 1     |
| 100.0–300.0     | 5   | 8     | 5     | 1     |
| 300.0–1000.0    | 5   | 8     | 5     | 1     |

$$\Delta\alpha^n(T_w, T_g, P_g L, F_{CO_2}, f_v L) = \frac{\Delta\alpha(T_w, T_g, P_g L, F_{CO_2}, f_v L) - \Delta\alpha_{\min}(T_w, T_g, F_{CO_2}, f_v L)}{\Delta\alpha_{\max}(T_w, T_g, F_{CO_2}, f_v L) - \Delta\alpha_{\min}(T_w, T_g, F_{CO_2}, f_v L)} \quad (8)$$

where  $\Delta\alpha_{\min}$  and  $\Delta\alpha_{\max}$  are the “excess absorptivity” evaluated at the minimum and maximum gaseous optical thickness of the considered region.

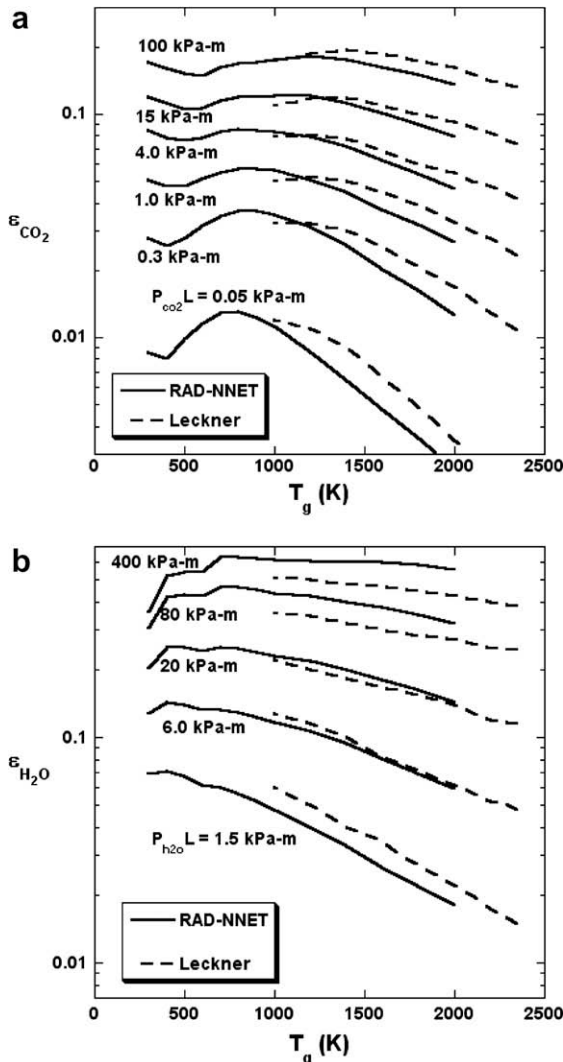


**Fig. 3.** (a) Total emissivity of CO<sub>2</sub>/air mixtures as a function of pressure-pathlength and gas temperature, comparing neural network with measurements by Leckner [21]. (b) Total emissivity of H<sub>2</sub>O/air mixtures as a function of temperature, comparing neural network with measurements by Leckner [21].

A three-layer network, as shown in Fig. 1, is used as a basis for the neural network development. The choice of a three-layer network is based the practical need to maintain the number of neurons needed for an accurate correlation to a reasonable value (say, less than 20). Numerical experiments show a three-layer structure is adequate for the current set of absorptivity data under consideration for all optical thickness regions. A “hyperbolic tangent sigmoid” function is used as the transfer function for the first two layers while a linear transfer function is used for the third layer. Using the Levenberg–Marquardt algorithm [11], a neural network with a set of  $S_1$ ,  $S_2$  and  $S_3$  neurons in the three-layer can be “trained” to yield the values of the three weight matrices  $\bar{W}^1$ ,  $\bar{W}^2$ ,  $\bar{W}^3$  and three bias vectors  $\bar{b}^1$ ,  $\bar{b}^2$ ,  $\bar{b}^3$  which would minimize the error between the network prediction and actual data. For the current neural network, the output vector is a scalar (absorptivity) and therefore  $S_3 = 1$ . Mathematically, the predicted value of the normalized output,  $a^3$ , for a gi-

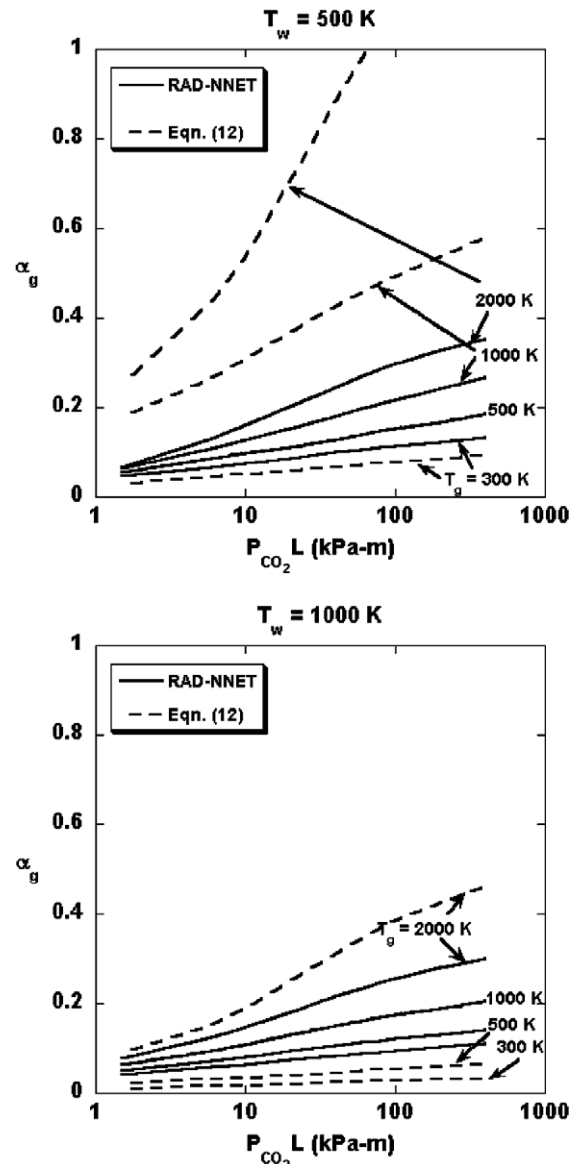


**Fig. 4.** Comparison between RAD-NNET and Eq. (12) in the absorptivity prediction for a CO<sub>2</sub>/N<sub>2</sub> mixture. (Note: the gas emissivity predicted by RAD-NNET is used in the evaluation of Eq. (12))

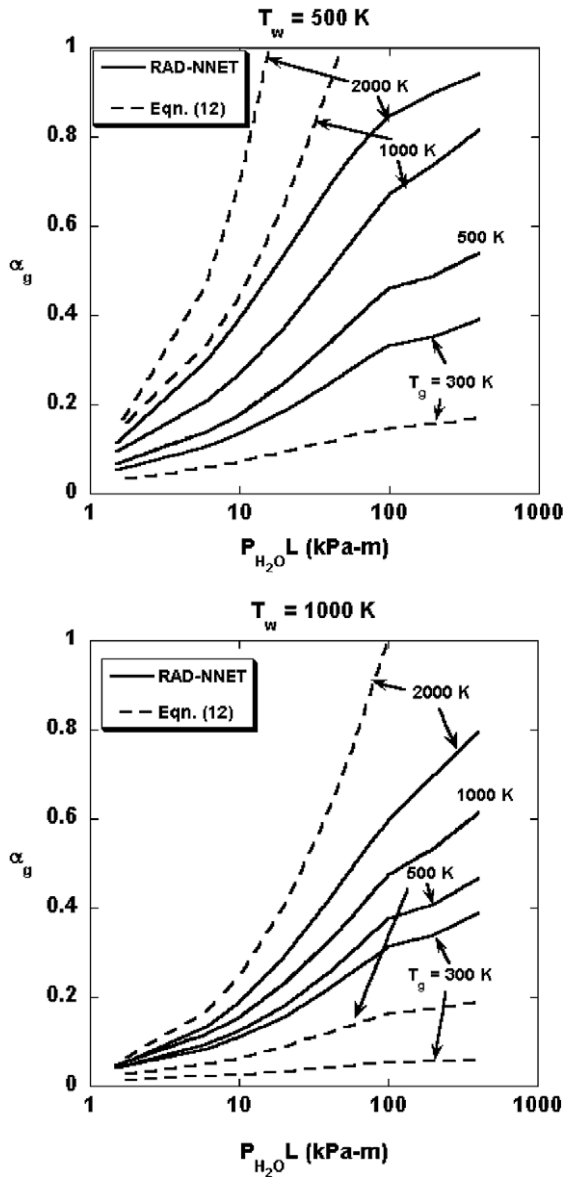


Fig. 5. Comparison between RAD-NNET and Eq. (12) in the absorptivity prediction for a H<sub>2</sub>O/N<sub>2</sub> mixture. (Note: the gas emissivity predicted by RAD-NNET is used in the evaluation of Eq. (12))

ven normalized input vector  $\vec{p}$  with the currently selected set of transfer function, is given by

$$a^3 = \sum_{i=1}^{S_3} a_i^2 W_i^3 + b^3 \quad (9)$$

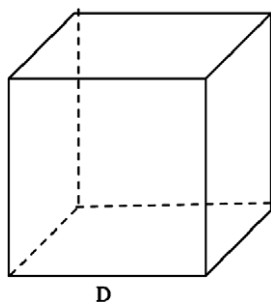


Fig. 6. Cubical enclosure with characteristic dimension  $D$  used in the evaluation of  $\tau_{pp}$  and  $\tau_{pd}$ .

with

$$a_i^2 = \tanh \left[ \left( \sum_{j=1}^{S_1} W_{ij}^2 a_j^1 \right) + b_i^2 \right], \quad i = 1, \dots, S_2 \quad (10)$$

$$a_i^1 = \tanh \left[ \left( \sum_{j=1}^N W_{ij}^1 p_j \right) + b_i^1 \right], \quad i = 1, \dots, S_1 \quad (11)$$

and  $N$  being the dimension of the normalized input vector. Results show that the “training” of the network was easily accomplished using standard MATLAB program in a PC. All numerical data are simulated to within a relative error of less than 0.5%. A comparison between the neural network prediction and the RADCAL results for a typical region is shown in Fig. 2. Dimensions of the weighted matrices and bias vectors for the 11 neural networks are summarized in Tables 1 and 2. Numerical values of neural networks are available to readers upon request.

In general, the accuracy of RAD-NNET is expected to be identical to that of RADCAL, which is known to be quite adequate for applications in combustion. For example, a comparison between RAD-NNET and some emissivity data for a CO<sub>2</sub>/N<sub>2</sub> mixture and H<sub>2</sub>O/N<sub>2</sub>

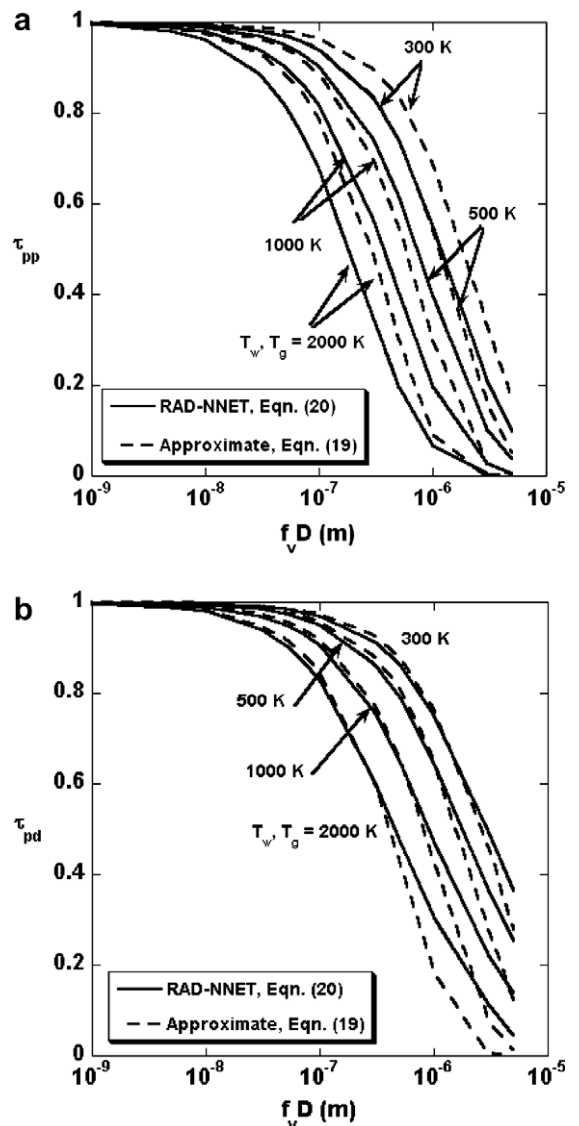


Fig. 7. Average transmissivity between two parallel surfaces and two adjacent surfaces in a cubical enclosure containing soot with various volume fraction, as predicted by Eqs. (19) and (20).

mixture [21] is illustrated by Fig. 3a, 3b. The agreement is excellent over a large range of optical thicknesses. Comparison with other available data [22,23] also shows similar agreement. Since RADCAL is based on direct integrations of the narrow-band spectral line, the same order of accuracy is expected for RAD-NNET in its prediction of absorptivity of a  $\text{CO}_2/\text{H}_2\text{O}/\text{N}_2/\text{soot}$  mixture, accounting for the overlap of absorption bands of  $\text{CO}_2$  and  $\text{H}_2\text{O}$ , the continuous absorption by soot, as well as the combined effect of the emitter's temperature  $T_w$  and the mixture temperature  $T_g$ .

### 3. Applications

The potential application of RAD-NNET is quite extensive. Due to its simplicity and accuracy, RAD-NNET can be readily implemented in any CFD calculations to simulate the effect of radiative absorption, provided the assumption of a homogeneous absorbing media between the emitter and the absorber can be justified. For non-uniform or non-isothermal media, RAD-NNET can be combined with existing inhomogeneous models such as the Curtis–

Godson approximation [24] to provide effective simulation of radiative absorption. For situations in which the Curtis–Godson approximation and other approximate inhomogeneous models are not applicable, an extended version of RAD-NNET can be readily generated using RADCAL to generate the “exact” numerical data for absorption by the considered inhomogeneous media. Indeed, this effort to extend RAD-NNET is currently under consideration and will be presented in future publications.

In the present work, the focus of the application of RAD-NNET is to rigorously assess the accuracy of some commonly accepted approximations used in the evaluation of radiative heat transfer in practical engineering systems. It is interesting to note that, until now, many of these approximations are used routinely in the engineering calculations without mathematical validation.

The first area in which empirical expressions and approximations are commonly used is in the evaluation of absorptivity. Since gas absorption data are generally presented in terms of emissivity, the evaluation of absorptivity by a gas mixture at temperature  $T_g$  for radiation emitted from a source of different temperature  $T_w$  is

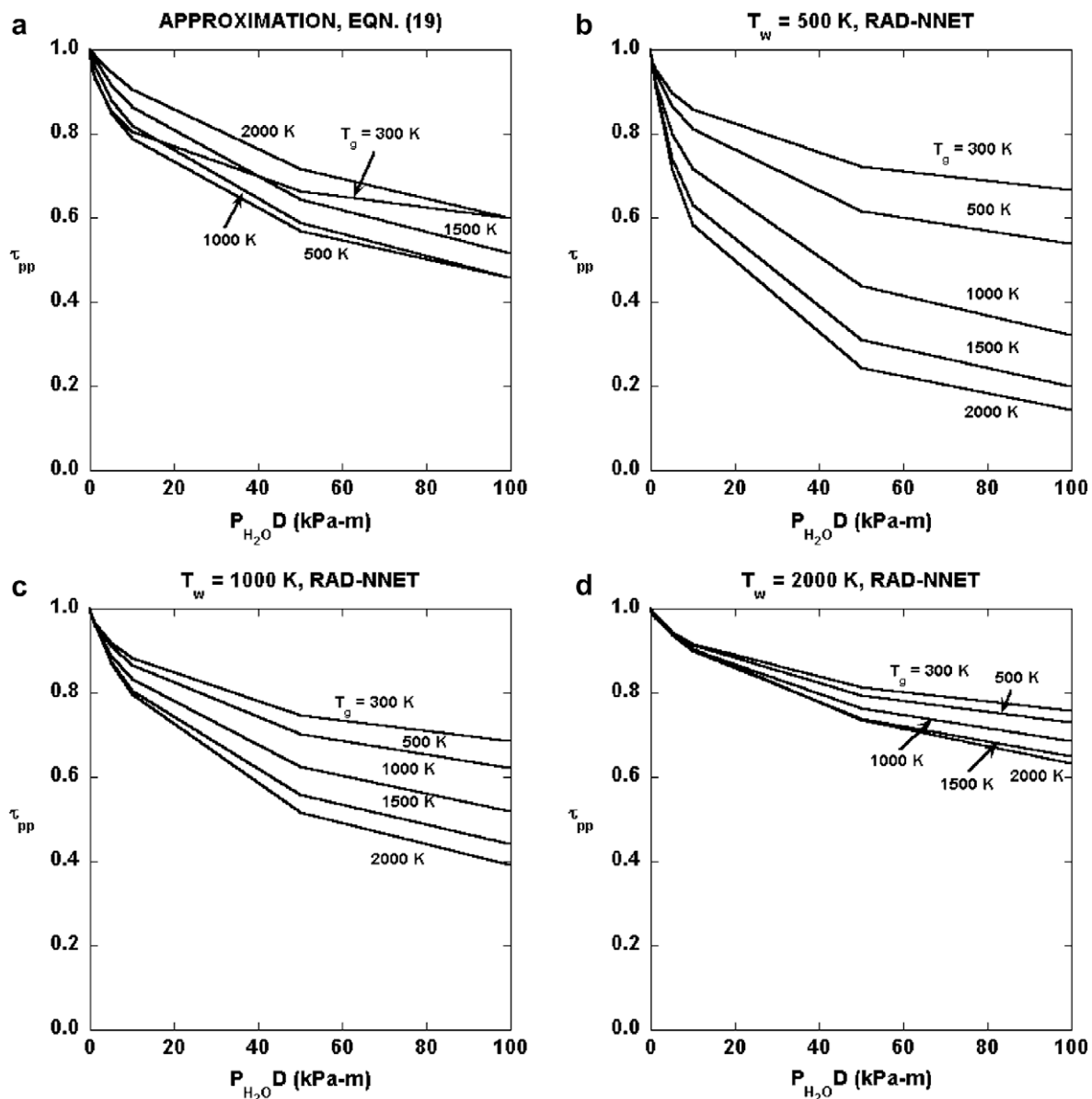


Fig. 8. Average transmissivity between two parallel surfaces in a cubical closure containing a  $\text{H}_2\text{O}/\text{N}_2$  mixture, as predicted by Eqs. (19) and (20).

difficult for practicing engineers who do not have the necessary skills or computational resources required for a detailed numerical calculation. Currently, a common approach is to utilize an empirical expression introduced more than forty years ago [25], which estimates the absorptivity from the gas emissivity by

$$\alpha_g = \varepsilon_g \left( \frac{T_g}{T_w} \right)^{1.5} \quad (12)$$

Comparisons between RAD-NETT and the approximate absorptivity as predicted by Eq. (12) for different emitter temperature  $T_w$  for a  $\text{CO}_2/\text{N}_2$  mixture and  $\text{H}_2\text{O}/\text{N}_2$  mixture are shown in Figs. 4 and 5. It is apparent that while Eq. (12) yields the correct qualitative behavior that the absorptivity increases with increasing gas temperature  $T_g$ , the approximation generally has significant error (higher than 100% and up to 1000%) and cannot be used reliably in any engineering calculations.

Another area of radiation heat transfer in which empirical and semi-empirical approximations are used extensively is in the evaluation of transmission/absorption by non-gray gases in multi-dimensional systems. It is important to note that even in a

simplified model such as a one-zone model with a homogeneous gas mixture, the radiative transfer to and from each boundary is three-dimensional and depends strongly on geometry. Without much mathematical validation, a commonly used approximate approach is to use the one-dimensional expression for gas emissivity and the concept of mean beam length of a gas volume to determine an “effective” absorption coefficient for the considered medium. For two surface elements on the boundary of the gas volume, an effective transmissivity is then evaluated based on an “average” distance between the two surfaces.

Specifically in the approximation, the total emissivity of the gas/soot mixture,  $\varepsilon_T$ , is first evaluated by

$$\varepsilon_T = \varepsilon_g + \varepsilon_s - \varepsilon_g \varepsilon_s \quad (13)$$

where  $\varepsilon_g$  is the gas emissivity which can be obtained from one-dimensional empirical correlations or emissivity charts based on a mean beam length of the emitting/absorbing volume given by

$$L_m = 3.6 \frac{V}{A} \quad (14)$$

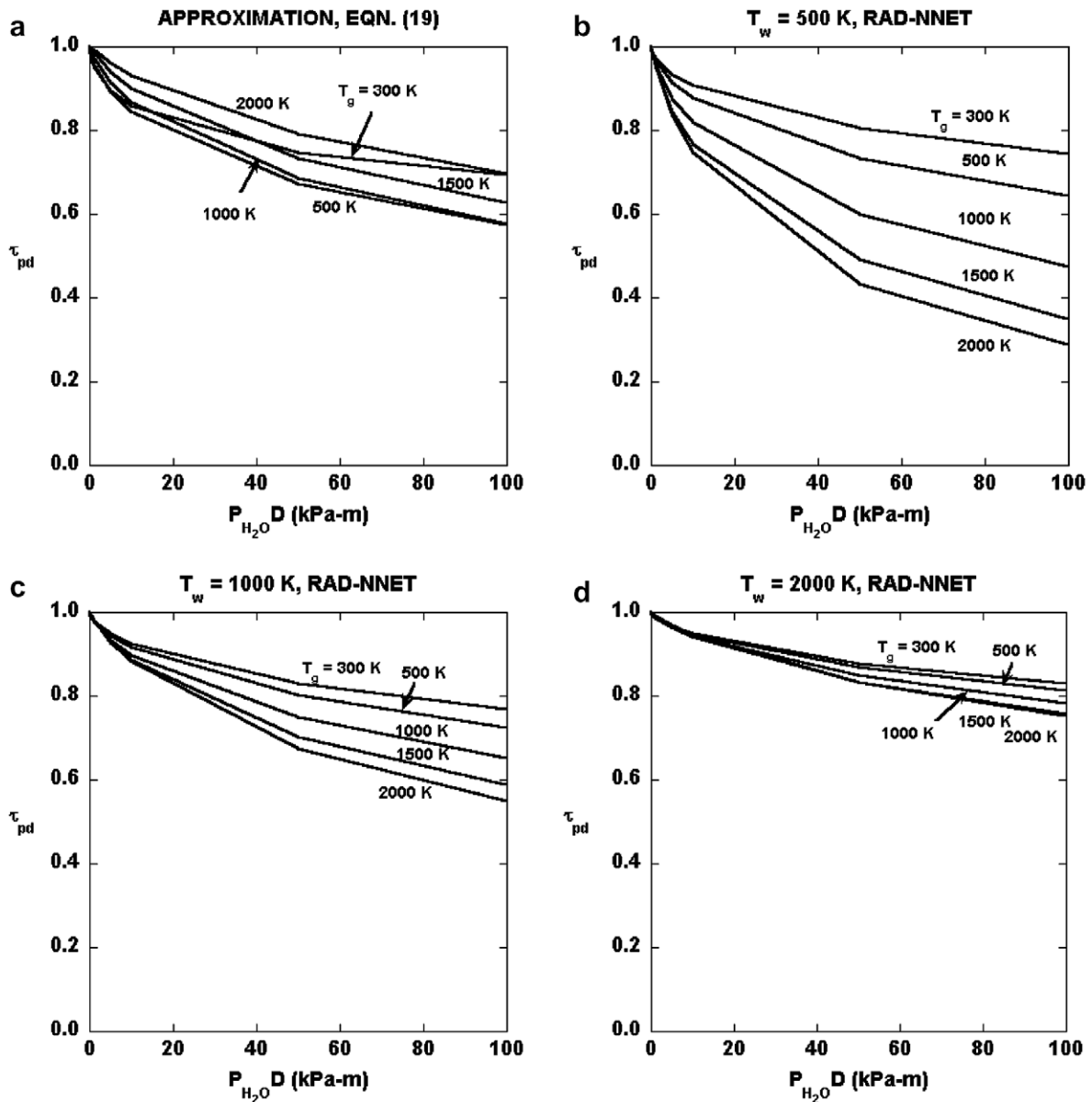


Fig. 9. Average transmissivity between two adjacent surfaces in a cubical closure containing a  $\text{H}_2\text{O}/\text{N}_2$  mixture, as predicted by Eqs. (19) and (20).

with  $V$  and  $A$  being the volume and surface area of the mixture, respectively. The soot emissivity,  $\epsilon_s$ , is evaluated by the following approximate expression

$$\epsilon_s = 1 - e^{-KL_m} \tag{15}$$

with

$$K = 3.6 \frac{cT_g}{C_2} \tag{16}$$

Eqs. (15) and (16) have been demonstrated to be an accurate approximation of Eq. (6) [26]. An effective absorption coefficient for the mixture,  $a_T$ , is then introduced as

$$a_T = -\frac{\ln(1 - \epsilon_T)}{L_m} \tag{17}$$

For two black surfaces,  $A_1$  and  $A_2$  situated at the boundary of the mixture volume, the radiative heat transfer is written as

$$Q_{1-2} = \sigma T_1^4 A_1 F_{12} \tau_{12} \tag{18}$$

where  $F_{12}$  is the exchange factor between the two surfaces and  $\tau_{12}$  is the average transmissivity between the two surface given by

$$\tau_{12} = e^{-a_T L_{12}} \tag{19}$$

In Eq. (19), the length scale  $L_{12}$  is typically taken to be the center-to-center distance between the two surface. The approximation, as represented by Eq. (13) through (19), is used as a “reasonable” procedure to estimate the radiative heat transfer through a non-gray gas/soot mixture in many existing CFD codes (for example, Refs. [6], [7] and [10]).

Since the total absorptivity of a gas/soot mixture can be evaluated accurately and efficiently with RAD-NNET, the average transmissivity can be evaluated quite conveniently by a direct numerical integration as follow:

$$\tau_{12} = \frac{1}{A_1 F_{12}} \int_{A_1} \int_{A_2} \frac{\cos \theta_1 \cos \theta_2 [1 - \alpha(T_w, T_g, P_g L, F_{CO_2}, f_v L)]}{\pi L^2} dA_2 dA_1 \tag{20}$$

where  $L$  is the physical pathlength between the two differential areas and  $\theta_1, \theta_2$  are the angles between the line of sight and the unit

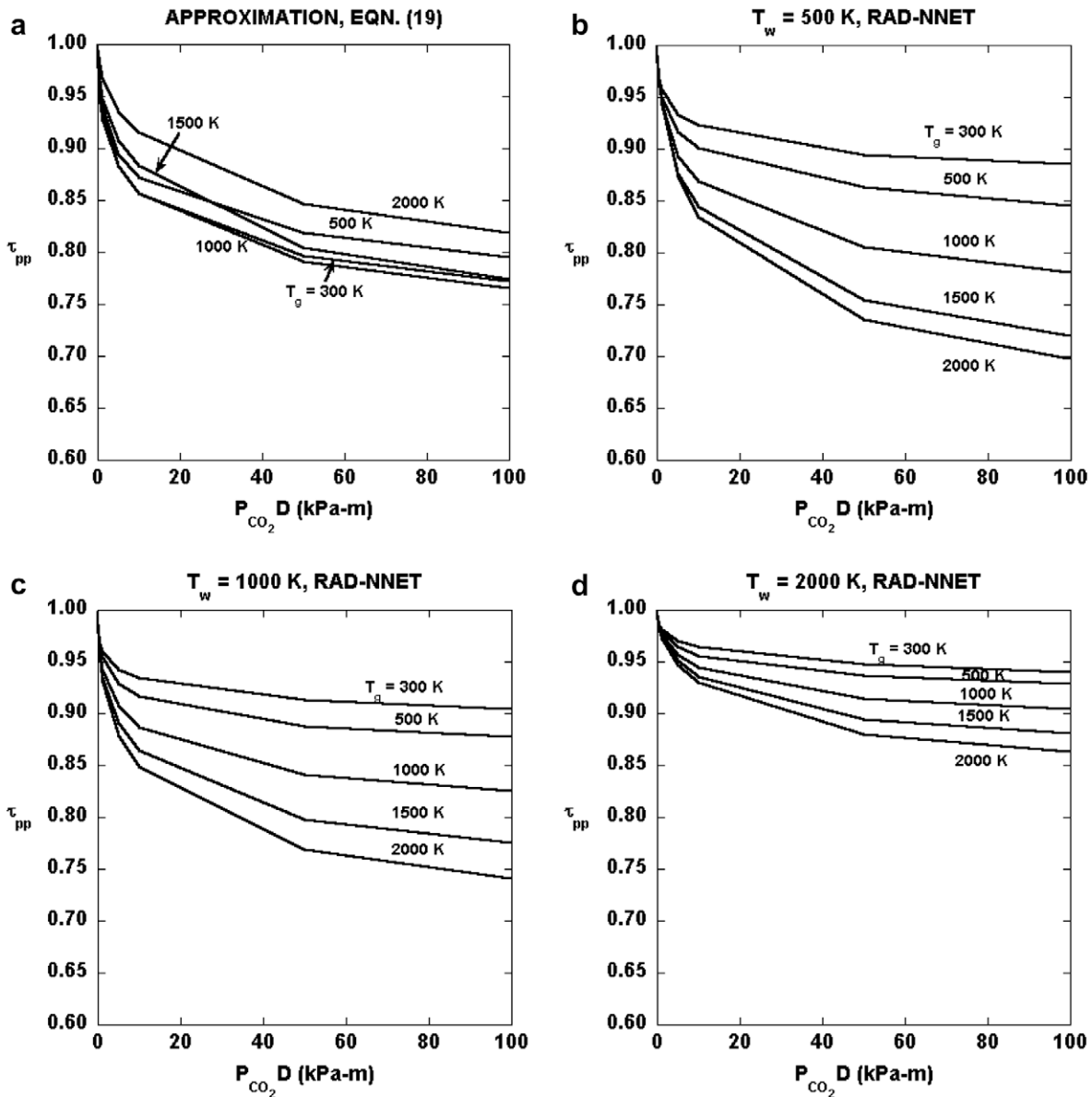


Fig. 10. Average transmissivity between two parallel surfaces in a cubical closure containing a CO<sub>2</sub>/N<sub>2</sub> mixture, as predicted by Eqs. (19) and (20).

normal of the two differential areas. Eq. (20) can now be used to assess the accuracy of Eq. (19) for various mixture conditions and geometric configurations.

Consider a cubical enclosure with dimension  $D$  as shown in Fig. 6. Let  $\tau_{pp}$  and  $\tau_{pd}$  be the average transmissivity between two parallel and two adjacent surfaces respectively. The evaluation of these transmissivities by Eqs. (19) and (20) for an enclosure containing only soot with various volume fractions are presented in Fig. 7a and 7b. Since Eq. (19) is evaluated at the mixture temperature  $T_g$  and the soot absorption is only a function of the emitter temperature  $T_w$ , Eq. (19) will always lead to significant error when  $T_g \neq T_w$ , data with  $T_w = T_g$  only are shown in Fig. 7a and 7b. It is interesting to note that in the limiting case with  $T_g = T_w$ , the transmissivity predicted by Eq. (19) can still have significant error, particularly in  $\tau_{pp}$ . This is due to the error of using the effective mean beam length in the evaluation of the effective absorption coefficient. Physically, a significant fraction of the radiative energy transmitted between two parallel surface must propagate through a distance larger than  $D$ . The mean beam length, as evaluated by

Eq. (14), is  $0.6D$ . This leads to an underestimate of the soot absorption, leading to a larger value of the transmissivity.

Results for the two transmissivities for  $\text{CO}_2/\text{N}_2$  and  $\text{H}_2\text{O}/\text{N}_2$  mixtures with various concentration and different temperatures are shown in Figs. 8–11. To eliminate any source of disagreement due to the use of different correlations, RAD-NNET is used in the evaluation of gas emissivity in Eq. (13). The error of using Eq. (19) is clearly quite substantial. Note that the approximation also fails to capture the general qualitative trend of decreasing gas absorptivity with increasing gas temperature (at a fix emitter temperature). This error can have a significant impact in the prediction of the transient behavior in many practical combustion scenarios such as the heat transfer between walls during the growth of a fire. When  $T_g = T_w$ , a direct comparison between the approximate results with the RAD-NNET results presented in these figures also shows significant differences.

In general, results presented in Fig. 7 through 11 show that the approximation, as represented by Eqs. (13) through (19), does not yield accurate prediction of the average transmissivity for a general

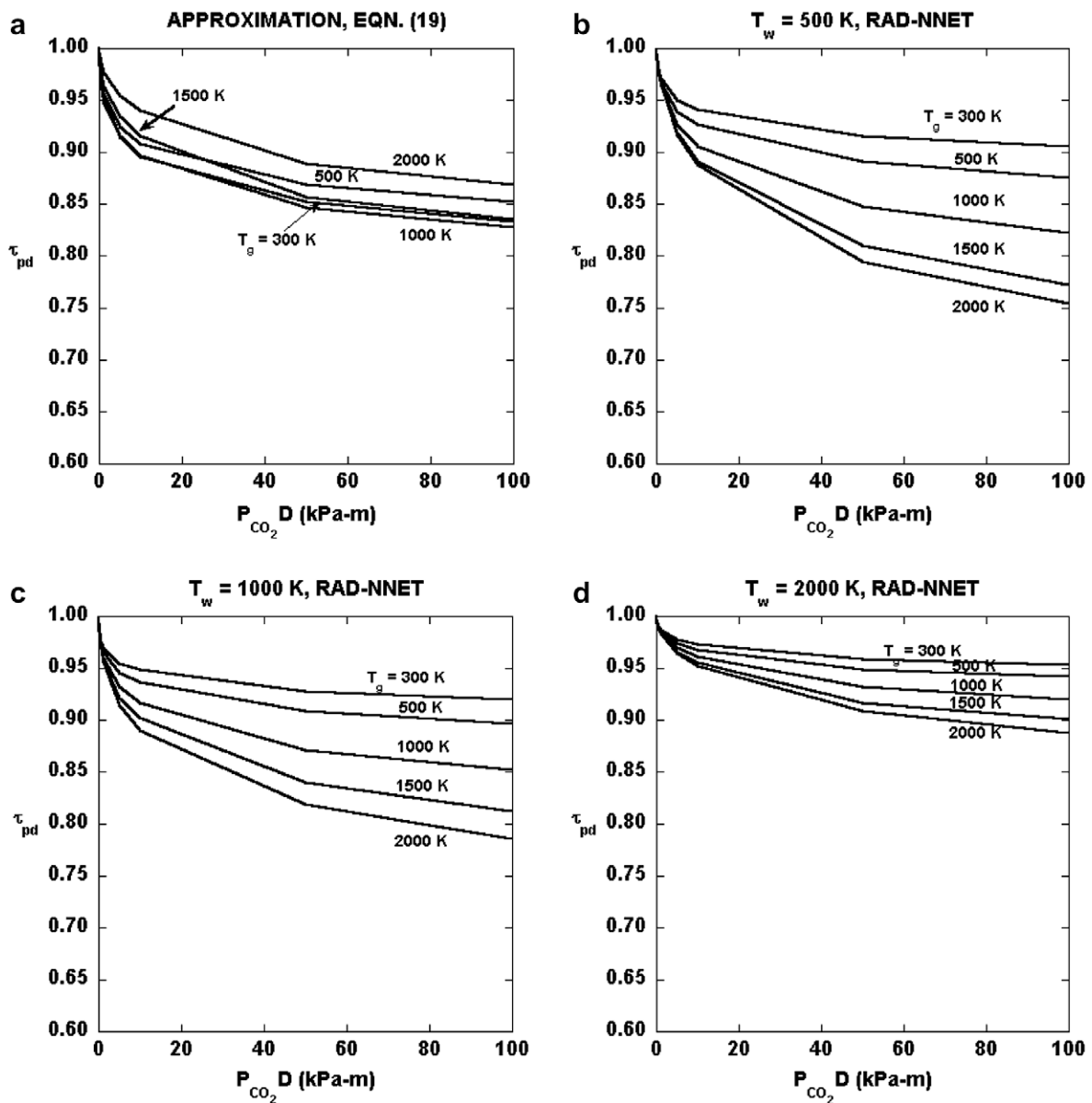


Fig. 11. Average transmissivity between two adjacent surfaces in a cubical closure containing a  $\text{CO}_2/\text{N}_2$  mixture, as predicted by Eqs. (19) and (20).

soot/CO<sub>2</sub>/H<sub>2</sub>O/N<sub>2</sub> combustion mixture and should not be used in practical engineering design/safety calculations.

#### 4. Conclusion

Neural network is shown to be an effective tool to allow data (numerical or experimental) of complex physical phenomenon such as radiative heat transfer to be utilized accurately and efficiently in a practical engineering calculation. A neural network RAD-NNET, for the radiative absorptivity of an isothermal combustion mixture is developed based on numerical data generated by RADCAL. As an example of implementation, the network is applied to assess the accuracy of two widely accepted approximation approaches used in the evaluation of radiative absorption of combustion media. Comparisons show that these two approaches are highly accurate.

For non-isothermal, inhomogeneous media, RAD-NNET can be combined with existing models such as the Curtis–Godson approximation [24] to accurately simulate the radiative absorption. For general applications, it is also important to develop a neural network for average absorptivity of a “gas” volume due to emission by the surrounding medium and boundaries. This effort, which will be formulated in the format of generalized exchange factors introduced in recent works [27,28], is current under way and will be reported in future publications.

#### References

- [1] R. Siegel, J. Howell, *Thermal Radiation Heat Transfer*, fourth ed., Taylor and Francis, New York, 2002.
- [2] M.F. Modest, *Radiative Heat Transfer*, second ed., Academic Press, 2003.
- [3] C. Ludwig, W. Malkmus, J. Reardon, J. Thomson, *Handbook of Infrared Radiation from Combustion Gases*, NASA-SP-3080, 1973.
- [4] W.L. Grosshandler, RADCAL, A Narrow-Band Model for Radiation Calculations in a Combustion Environment, NIST-TN-1402, National Institute of Standard and Technology, April 1993.
- [5] D.V. Walters, R.O. Buckius, Monte Carlo method for radiative heat transfer in scattering media, *Ann. Rev. Heat Transfer*, CRC Press, Boca Raton, FL, 1994. pp. 131–176.
- [6] W.W. Jones, R.D. Peacock, G.P. Forney, P.A. Reneke, CFAST: Consolidated Model of Fire Growth and Smoke Transport (Version 5), Technical Reference Guide, NIST-SP-1030, National Institute of Standard and Technology, October, 2004.
- [7] K. McGrattan, S. Hostikka, J. Floyd, H. Baum, R. Rehm, *Fire Dynamics Simulator (Version 5)*, Technical Reference Guide, NIST Special Publication 1018-5, National Institute of Standard and Technology, October 1, 2007.
- [8] D.K. Edward, Molecular gas band radiation, in: T.F. Irvine Jr., J.P. Hartnett (Eds.), *Advances in Heat Transfer*, vol. 12, Academic Press, New York, 1976, pp. 115–193.
- [9] H.C. Hottel, A.F. Sarofim, *Radiative Transfer*, McGraw Hill, New York, 1967.
- [10] G.P. Forney, Computing Radiative Heat Transfer in a Fire Zone Model, NISTTR-4709, National Institute of Standard and Technology, November 1991.
- [11] M.T. Hagen, H.B. Demuth, M. Beale, *Neural Network Design*, PWB Publishing Company, Boston, 1995.
- [12] DARPA Neural Network Study, Lexington, MA: MIT Lincoln Laboratory, 1988. (Chapter 1).
- [13] J.C. Bokar, The estimation of spatially varying albedo and optical thickness in a radiating slab using artificial neural network, *Int. Commun. Heat Mass Transfer* 26 (3) (1999) 359–367.
- [14] C. Cornet, H. Isaka, B. Guillemet, F. Szczap, Neural network retrieval of cloud parameters on inhomogeneous cloud of multispectral and multiscale radiance data: feasibility study, *J. Geophys. Res. – Atmos.* 109 (D12) (2004). Art. No. D12203, 2004.
- [15] M. Deiveegan, C. Balaji, S.P. Venkateshan, Comparison of various methods for simultaneous retrieval of surface emissivities and gas properties in gray participating media, *ASME J. Heat Transfer* 128 (8) (2006) 829–837.
- [16] H. Kagiwada, R. Kalaba, S. Timko, S. Ueno, Associate memories for system identification – inverse problems in remote sensing, *Math. Comput. Modell.* 14 (1990) 200–202.
- [17] H. Schiller, R. Doerffer, Neural network for emulation of an inverse model – operational derivation of case II water properties from MERIS data, *Int. J. Remote Sens.* 20 (9) (1999) 1735–1746.
- [18] F. Badran, S. Thiria, Multilayer perceptrons: from nonlinear regression to inverse problems, *J. Phys. IV* 12 (PR1) (2002) 157–188.
- [19] A. Pacheco-Vega, G. Diaz, M. Sen, K.T. Yang, R.L. McClain, Heat transfer prediction in humid air–water heat exchangers using correlations and neural network, *ASME J. Heat Transfer* 123 (2) (2001) 348–354.
- [20] K.M. Hornik, M. Stinchcombe, H. White, Multilayer feedforward networks are universal approximators, *Neural Netw.* 2 (5) (1989) 359–366.
- [21] B. Leckner, Spectral and total emissivity of water vapor and carbon dioxide, *Combust. Flame* 19 (1972) 33–48.
- [22] P. Docherty, Prediction of gas emissivity for a wide range of conditions, in: *Proceeding of the 7th International Heat Transfer Conference*, vol. R5, 1982, pp. 481–485.
- [23] H.C. Hottel, R.B. Egbert, *Trans. Am. Inst. Chem. Eng.* 38 (1942) 531–565.
- [24] R.M. Goody, *Atmospheric radiation, Theoret. Basis*, vol. 1, Clarendon Press, Oxford, 1964.
- [25] A.H. Lefebvre, M.V. Herbert, Heat transfer processes in gas–turbine combustion chambers, *Proc. Inst. Mech. Eng.* 174 (1960) 463–473.
- [26] W.W. Yuen, C.L. Tien, A simple calculation scheme for the luminous-flame emissivity, in: *The 16th Symposium (International) on Combustion*, The Combustion Institute, 1977, pp. 1481–1487.
- [27] W.W. Yuen, Development of a multiple absorption coefficient zonal method for application to radiation heat transfer in multi-dimensional inhomogeneous non-gray media, *Numer. Heat Transfer B* 49 (2) (2006) 89–103.
- [28] W.W. Yuen, Definition and evaluation of mean beam lengths for applications to multi-dimensional radiative heat transfer: a mathematically self-consistent approach, *ASME J. Heat Transfer* 130 (11) (2008) 114507.